Stress growth and relaxation of dendritically branched macromolecules in shear and uniaxial extension

Huang, Qian; Costanzo, S.; Das, C.; Vlassopoulos, Dimitrios

Published in:
Journal of Rheology

Link to article, DOI:
10.1122/1.4966040

Publication date:
2017

Document Version
Peer reviewed version

Stress growth and relaxation of dendritically branched macromolecules in shear and uniaxial extension

Q. Huang[1], S. Costanzo[2,3], C. Das[4], D. Vlassopoulos[2,3]

(1) Department of Chemical and Biochemical Engineering, Technical University of Denmark (DTU), Lyngby 2800 Kgs., Denmark.
(2) Institute of Electronic Structure & Laser, Foundation for Research and Technology Hellas (FORTH), Heraklion, Crete 70013, Greece.
(3) Department of Materials Science & Technology, University of Crete, Heraklion, Crete 71003, Greece.
(4) School of Mathematics, University of Leeds, Leeds LS2 9JT, United Kingdom

Abstract

We present unique nonlinear rheological data of well-defined symmetric Cayley-tree poly(methyl methacrylates) in shear and uniaxial extension. Earlier work has shown that their linear viscoelasticity is governed by the hierarchical relaxation of different generations, whereas the segments between branch points are responsible for their substantial strain hardening as compared to linear homopolymers of the same total molar mass at the same value of imposed stretch rate. Here, we extend that work in order to obtain further experimental evidence that will help understanding the molecular origin of the remarkable properties of these highly branched macromolecules. In particular, we address three questions pertinent to the specific molecular structure: (i) is steady state attainable during uniaxial extension? (ii) what is the respective transient response in simple shear? and (iii) how does stress relax upon cessation of extension or shear? To accomplish our goal we utilize state-of-the-art instrumentation, i.e., filament stretching rheometry (FSR) and cone-partitioned plate (CPP) shear rheometry for polymers with 3 and 4 generations, and complement it with state-of-the-art modeling predictions using the Branch-on-Branch (BoB) algorithm. The data indicates that the extensional viscosity reaches a steady state value, whose dependence on extension rate is identical to that of entangled linear and other branched polymer melts. Nonlinear shear is characterized by transient stress overshoots and the validity of the Cox-Merz rule. Remarkably, nonlinear stress relaxation is much broader and slower in extension compared to shear. It is also slower at higher generation, and rate-independent for rates below the Rouse rate of the outer segment. For extension, the relaxation time is longer than that of the linear stress relaxation, suggesting a strong ‘elastic memory’ of the material. These results are

described by BoB semi-quantitatively, both in linear and nonlinear shear and extensional regimes. Given the fact that the segments between branch points are less than 3 entanglements long, this is a very promising outcome that gives confidence in using BoB for understanding the key features. Moreover, the response of the segments between generations controls the rheology of the Cayley trees. Their substantial stretching in uniaxial extension appears responsible for strain hardening, whereas coupling of stretches of different parts of the polymer appears to be the origin of the slower subsequent relaxation of extensional stress. Concerning the latter effect, for which predictions are not available, it is hoped that the present experimental findings and proposed framework of analysis will motivate further developments in the direction of molecular constitutive models for branched and hyperbranched polymers.

I. Introduction

The use of model polymers of well-defined architecture is important in probing molecular rheology [1–4]. Indeed, substantial progress has been made in decoding the linear viscoelasticity of model branched polymers (such as combs or pom-pom-like macromolecules), and more recently their nonlinear response in shear and extension. The rheological properties of model polymers provide profound implications in finessing molecular models and improving material performance in technological applications [5–15]. Focusing on the nonlinear rheology of comb polymers, one important consequence of the recent progress in experimental extensional and shear rheology is the quantitative assessment of the role of dynamic dilution in transient strain hardening and stress overshoot, respectively. Moreover, it has been demonstrated that, still using the comb paradigm, introducing long-chain branching induces strain hardening in start-up shear [9]. It is therefore evident that whereas branching is crucially important in processing, the exact role of number, size and distribution of branches is not fully quantified. We note that Nielsen et al. measured the transient response of model pom-pom polystyrenes [10] (which are a limiting case of combs with only two branch points at the ends of the backbone) and reported strong extension hardening, even at low deformation rates, due to the stretching of the backbone between the two branch points. The extensional viscosity reached steady state with values scaling with the extensional rate with a power exponent of about -0.5, in agreement with modelling predictions [10,16]. The latter were based on the concept of

internal chain pressure which counterbalances the contraction due to the applied deformation, [17,18] coupled with backbone tube dilation due to the earlier relaxation of the branches. These ideas were also implemented into the time marching algorithm by van Ruymbeke et al. 2010 [19,20] in order to predict the extension hardening of Cayley-tree poly(methyl methacrylates) of different generations. However, in the latter case, despite the very good predictions of transient stress growth coefficient, the experimental measurements were limited to maximum Hencky strains of 4 and in some cases, the steady state was not reached. Moreover, Marrucci and Ianniruberto suggested that the tube pressure is not a universal concept and proposed instead the idea of anisotropic monomeric friction as the main mechanism to account for the response of polymer melts and solutions in uniaxial extension [21–23]. An important element of the pom-pom model is the branch withdrawal at rates larger than the effective Rouse rate of the polymer. This was worked out for the case of multiple branches along the backbone, and a modified pom-pom model for combs captured the transient extensional data remarkably well [15]. In parallel, whereas experiments with well-defined branched polymers (such as combs) are absolutely necessary in order to elucidate the role of the molecular parameters (number, size and distribution of branches, distance between branch points) in the rheological response, the state of the art BoB model, developed for randomly branched polymers [24], can be adopted to well-defined branching in a straightforward way. In some specific situations, the complex transient response of combs can be described with simple models accounting for branch withdrawal and convective constraint release, but a universal constitutive model is far from reach. In addition, it is important to emphasize that nonlinear rheological experiments with polymer melts are far from non-trivial. Challenges of particular significance are the potential achievement of steady state in extension and associated ability to reach sufficiently high Hencky strains (above 4, as mentioned before) on one hand, and the occurrence of wall slip and edge fracture instabilities in shear on the other hand. Moreover, stress relaxation has emerged as an important experimental indicator of material performance baring information on the role of molecular structure on macroscopic response [25,26]. Hence, outstanding challenges remain in the field, on both experimental and modelling sides.

Recent advances in instrumentation have opened the route for obtaining high-quality experimental data, especially in nonlinear transient conditions. More specifically, the development of the filament stretching rheometer (FSR) allows the measurement of true stress in well-controlled uniaxial extension at large Hencky strains and that of stress

relaxation upon cessation of extension [25,27]. At the same time, the implementation of cone-partitioned plate (CPP) in rotational strain-controlled rheometry offers the ability to measure reliably transient shear stress over the largest possible range of shear rates [28–30]. It is therefore essential to combine novel macromolecular structures of relevance in processing and state of the art experimental tools in order to provide useful, reliable experimental information in different flow histories, towards a better understanding of the behaviour of complex polymers and a critical assessment of predictive models and their eventual improvement.

In this work, we address this challenge and present a combined set of accurate experimental data with a well-defined dendritically branched macromolecule of third and fourth generation subjected to both nonlinear shear and uniaxial extensional deformation, during both start-up and relaxation upon flow cessation. We compare these experimental data against modelling predictions using BoB. The choice of the particular Cayley-tree type of structure is motivated by the fact that it is an excellent model for investigating the hierarchical role of branches (with and without free ends, with varying number and molar mass) in rheology, and represents a next step in complexity from comb [19,31]. One well-known, albeit intriguing aspect of such macromolecules is their rather low zero-shear viscosity and larger level of extension hardening due to the fact that their very large total molar mass is split into multiple segments (hyperbranched), each having small molar mass. Here we present new data with Cayley tree poly(methacrylates) of generations 3 and 4 (section II), whose linear viscoelasticity and strain hardening was investigated before. We show, in particular, the transient extensional data with steady state values at large Hencky strains, respective transient shear data, the Cox-Merz representation, and the relaxation of extensional and shear stresses, along with the BoB predictions (section III). The key conclusions and implications of the work are summarized in the last section.

II. Materials and methods

II.1. Cayley-tree polymers: We used Cayley-tree poly(methyl methacrylates), PMMA, of generations 3 (code G3) and 4 (code G4). These dendritically branched macromolecules were synthesized anionically by Hirao and co-workers [32–36] using benzyl bromide moieties as coupling agents. Earlier rheological investigations were discussed by van

Ruymbeke et al. [19]. Each tree polymer consists of equal segments between generations (or with a free end at the highest generation). The number average molar mass of each segment is M_n=11,000 g/mol (i.e., 2.4 entanglements) and the polydispersity index M_w/M_n=1.02. Figure 1 below provides cartoon illustrations of the molecular structures of G3 and G4. Characterization of G3 and G4 can be found in Ref. [19] and [35,36]. Here we note that we performed size exclusion chromatography in fresh and used (after first stretching experiment) samples G4. The results from the analysis with the RI detector (not shown) show that there is a small fraction (about 6%) of larger molecules, which we call side-products, with an average molar mass of about 1340 kg/mol, i.e. double that of the main target product (see also Refs. [32–36]). Whereas these side-products have an influence on the linear viscoelasticity at very long times [19], at this small amount they do not affect the terminal response of the target dendritic molecules. This is also supported by earlier extensive work on structural and rheological analysis of branched polymers [2,19,37]. Furthermore, the used samples appear to contain slightly larger fraction of side-products (10%) but were perfectly soluble in good solvent chloroform. These facts, along with evidence from literature (for fractions of 15% of lower we can ignore their contribution to a first approach [37]), give confidence about the appropriateness of these samples for the present investigation (see also section III.1 below).

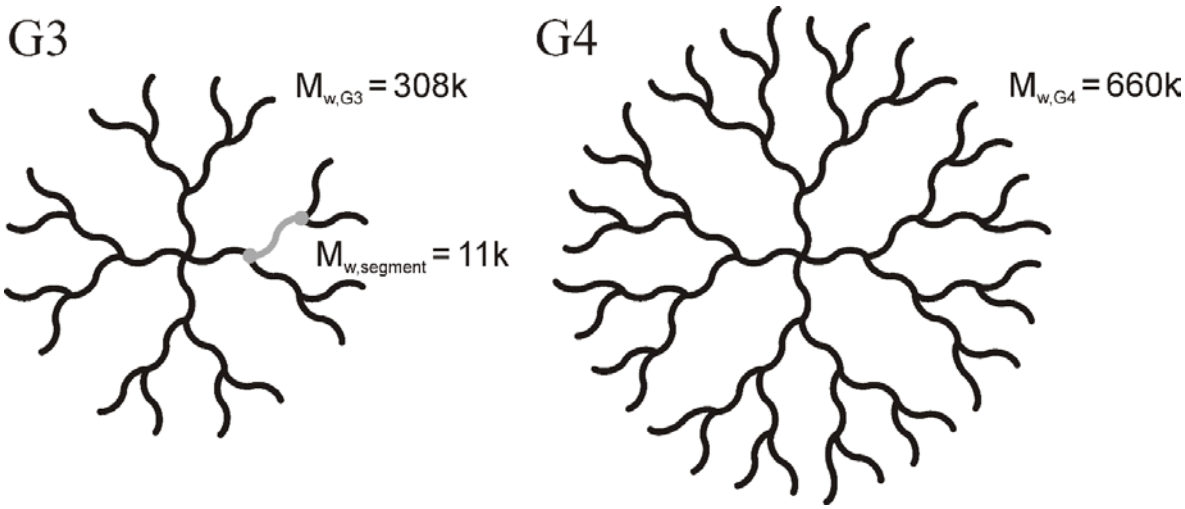

Figure 1: Illustration of Cayley tree polymers of 3 (G3) and 4 (G4) generations.

II.2. Sample preparation: Prior to molding the samples were dried in a vacuum oven at 90ºC for two to three days. The materials were then molded into cylindrical test specimens

using homemade vacuum molds (typically, between two Teflon discs). The amount of sample for each specimen was about 20–40 mg. The materials were pressed at approximately 170 ºC (the mold was put in a hot press with applied load of 0.4 tons). This protocol ensured that the samples were properly annealed. Given the low quantity of samples, the specimens for both extensional and shear measurements were reused when necessary, after a rheological test was completed. The recovered sample from the rheometer was remolded by using the same protocol described above. Possible degradation was checked before new rheological measurements via reproducibility of linear viscoelastic measurements and size exclusion chromatography.

II.3. Rheology:

II.3.1. Uniaxial extension: The extensional stress measurements were performed with a filament stretching rheometer (FSR) [27,38,39]. The molded specimens had a fixed radius of R_0=2.7mm. The initial length L_0 of the cylindrical test specimen was controlled by adding an appropriate mass of sample into the mold. The aspect ratio $\Lambda_0 = L_0 / R_0$ ranged between 0.41 and 0.56. The samples were pre-stretched to a radius R_p ranging from 1.2 to 2.4 mm at 180°C prior to the extensional experiments. After pre-stretching, the measurements were carried out in nitrogen atmosphere at the same temperature and the force $F(t)$ was measured by a load cell whereas the specimen diameter $2R(t)$ at the mid-filament plane was monitored by means of a laser micrometer. Note that during the startup of elongational flow, part of the force comes from the radial variation due to the shear component of the deformation field. This effect may be non-negligible for small strains only and in that case it is compensated by a correction factor. The Hencky strain ε_H and the mean value of the stress difference over the mid-filament plane can be calculated from $R(t)$ and *F(t)* as:

$$\varepsilon_H(t) = -2\ln\left(\frac{R(t)}{R_p}\right) \tag{1}$$

and

$$\left\langle \sigma_{zz} - \sigma_{rr} \right\rangle = \frac{F(t) - m_f g/2}{\pi R^2(t)} \frac{1}{1 + \left[R(t)/R_0\right]^{10/3} \exp\left(-\Lambda_0{}^3\right)/(3\Lambda_0{}^2)} \tag{2}$$

where m_f is the mass of the filament, and g is the gravitational acceleration. The stretch rate $\dot{\varepsilon} = d\varepsilon_H / dt$ can remain constant by means of a control scheme [38] and the extensional stress growth coefficient is defined as $\eta_{el}^{+} = \langle \sigma_{zz} - \sigma_{rr} \rangle / \dot{\varepsilon}$. In the stress relaxation phase following the startup of uniaxial extension, the mid-diameter of the filament is kept constant by the control scheme, giving $\dot{\varepsilon}$ = 0. The extensional stress decay coefficient is defined as $\eta_{el}^{-} = \langle \sigma_{zz} - \sigma_{rr} \rangle / \dot{\varepsilon}$, where $\dot{\varepsilon}$ is the strain rate in the startup of the flow.

II.3.2. Simple shear: Measurements were performed in a strain-controlled ARES rheometer (TA Instruments, USA) equipped with a force rebalance transducer (2KFRTN1). Linear and nonlinear measurements were performed with a homemade cone-partitioned plate (CPP) fixture in order to avoid experimental artefacts associated with edge fracture. The particular CPP used is described in detail in Costanzo et al. [30]. All tools used were made of stainless steel. The inner partition has a diameter of 6 mm while the outer partition has an inner diameter of 6.2 mm and an outer diameter of 20 mm. The role of the partition is to delay the onset of edge fracture propagating inside and protect the measured part of the sample (adhering to the inner plate). The cone used has an angle of 0.1 rad and a truncation of 51 μm. The CPP geometry was inserted into the ARES convection oven, hence a temperature control of ±0.1ºC was achieved. Nitrogen flow reduced the risk of degradation. The lowest attainable shear rate with this geometry was 0.01 s^{-1}. Nonlinear start-up tests with sample G3 were carried out at 180ºC. The measurements with sample G4 at the two lowest shear rates (0.001 and 0.003s^{-1}) were performed at 200ºC and then shifted to 180ºC using the horizontal shift factor of the linear viscoelastic data [19]; measurements at larger rates were performed at 180ºC.

II.4. Modeling: In view of the lack of mesoscopic models predicting the rheology of generic unentangled (or barely entangled, as here) branched polymers, we used the BoB model [8,24,40] in order to describe the flow properties of the Cayley tree polymers. Computational rheology [24,41,42] follows coupled relaxation in time of a numerical ensemble of molecules after a small, affine, step strain. For a Cayley tree molecule, the relaxation starts by arm retraction [43,44] of the outermost segments with one free end. The relaxed segments act like solvent for the yet to be relaxed segments [45], and thus coupling

the relaxation of all the molecules considered in the calculation. The inner segments can only relax (by Rouse-like explorations as described below) once the outer segments have relaxed completely and their relaxation is slowed due to the localized friction at the branch points (which is accounted for). Hence, inner segments become gradually available for branch-point withdrawal. The time at which certain part (of inner segment) becomes available for relaxation is assigned as its stretch relaxation time. Relaxation of such compound segments that contain one or more localized friction points is described by a multi-dimensional first-passage problem and is simplified by considering the portion of this compound arm that can move coherently with the chain end at a given time and assigning a dynamics to this effective pivot point of a compound segment [24]. Specifically, when the first two generations have relaxed, there are two localized friction points in the "compound" arm. We consider contour length fluctuations process in branch retraction that is limited to the length available via the above mentioned Rouse process. In general, the final unrelaxed material behaves like a linear polymer and the terminal relaxation is via reptation. However, for the symmetric molecules considered here, reptation plays no role. We used a value for the dilution exponent α=1 and branch point hopping parameter p^2=1/40. Concerning the latter, we note that it is significantly smaller than more commonly chosen value of p^2 = 1/12 [46,47], but this choice was found to simultaneously fit all rheological data of asymmetric star and other branched polymers [6,23,24,48,49]. Part of the reason for smaller value of the chosen parameter is because we consider that the friction from a relaxed side-arm is set by the tube diameter at the time-scale of branch-point retraction. The exact numerical value probably is of no great significance. Rather this is a fit parameter that would have been different, had we made different choices for complete branch retraction. Note that the default choice in BoB is to consider branch-point retraction only when the chain end visits the origin; in this work we consider complete retraction when the chain end reaches 0.15 times the current effective tube diameter. This change was necessary in order to describe both the resins with a single value of the entanglement molar mass. We have chosen this small value of effective entanglements as the criteria for complete branch-withdrawal to ensure that results for well entangled polymers remain unchanged.

For reasons still not fully resolved, small side-arms (of the order one entanglement or even less than an entanglement) have been found to provide significantly larger friction than tube theory predictions based on long side-arms [48,50]. Recent molecular dynamics results also suggest that entanglement constraints at the branch-points are stronger than

those for linear polymers [49]. For this reason, we have decided not to have a cut-off function at order one entanglement like in the hierarchical model [40,41]. Having a zero (as in the original BoB model) or a small value (as in the present work) allows us to predict rheology of branched polymers with segment lengths down to order one entanglement. To predict the nonlinear flow response, we resolve the linear relaxation as a set of pom-pom modes and the procedure is described in III.2.

III. Results and discussion

III.1. Linear viscoelasticity. As reference, we present first the linear viscoelastic (LVE) data of the two samples in Figure 2. The master curves are taken from van Ruymbeke et al. (2010) and shifted to the reference temperature T_{ref} =180ºC and are shown in separate plots (Figs. 2a and 2b for G3 and G4, respectively) in order to appreciate the BoB predictions. The shift factors are discussed in reference [19]. In fact, we have re-measured the frequency-dependent dynamic moduli at 180ºC and our results were identical to those of van Ruymbeke et al. (2010), hence confirming that the samples were not degraded. We remind here the main outcome from the linear data (not shown in the separate plots of Fig. 2): time-temperature superposition works remarkably well, high-frequency data collapse for G3 and G4 having the same glass temperature (of about 100ºC), the plateau G' (corresponding to about 10^2 rad/s) is identical for the two samples and typical of that of linear atactic PMMA. Continuous decrease of G' with decreasing frequency reflects the dynamic dilution due to relaxation of branches of different generations from outer proceeding inwards [19,44]. Finally, the terminal relaxation of G4 is slower than that of G3. In particular, the respective terminal moduli crossover frequencies are 0.005 rad/s and 0.03 rad/s. Regarding the nonlinear rheology that follows, the imposed shear and extensional rates cover the range from $3x10^{-1}$ to 10^{-3} s^{-1}. This is a rather wide range given the experimental limitations, and at the same time very useful as it encompasses the transition from rubbery (deformed polymers) to terminal response, respectively, in Figure 2.

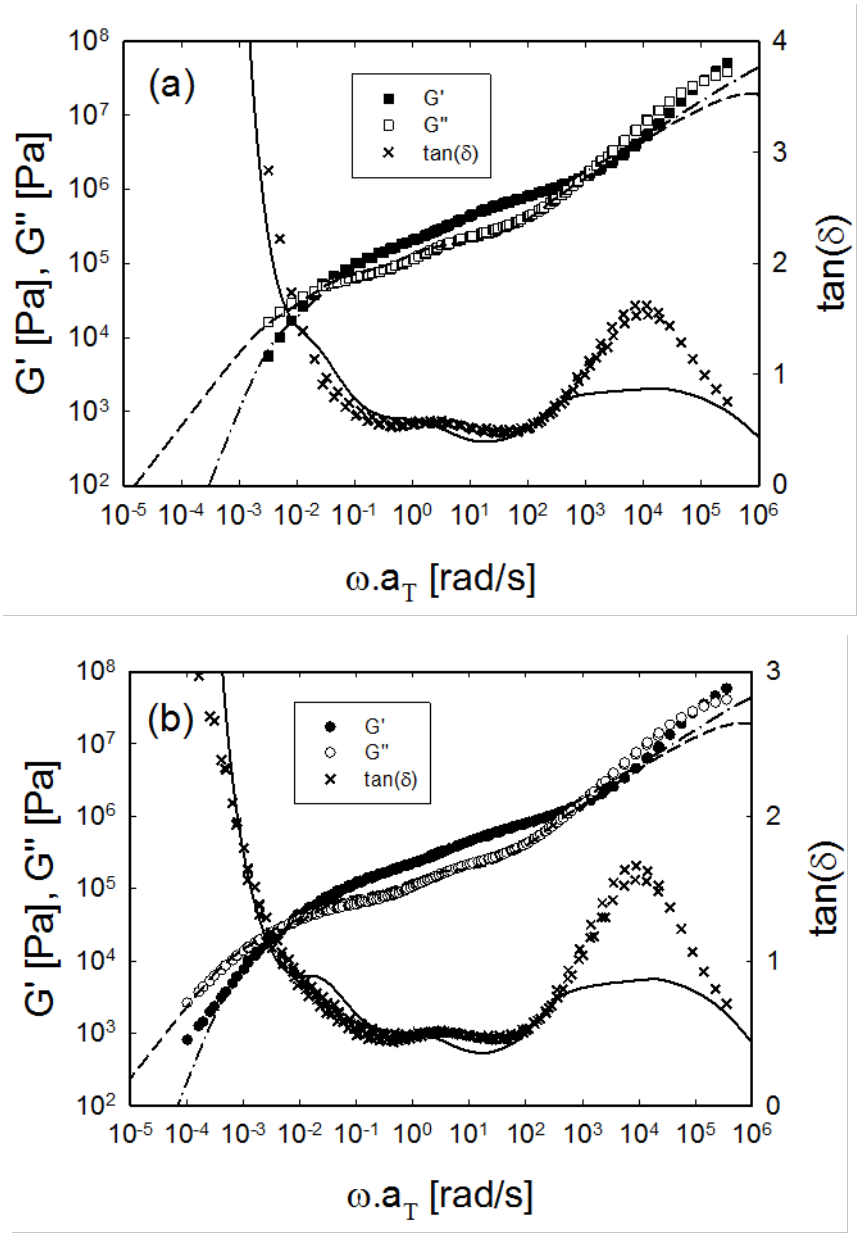

Figure 2: Linear viscoelastic master curves from van Ruymbeke et al. [19], depicting G' (closed circles), G'' (open circles) and tan(δ) (crosses) versus shifted frequency ($\omega.a_T$) at a reference temperature T_{ref}=180ºC for G3 (a) and G4 (b). For both graphs, black lines are predictions from BoB model (G', dash-dotted line; G'', dashed line; tan(δ), solid line).

For BoB modelling, we chose M_e=5000 g/mol (slightly higher than that reported in [19]) and τ_e=2.5 ms (consistent with [19] when the experimental temperature of 180ºC is considered). The plateau modulus is independently set at 0.98 MPa. Though the 'bare' molar masses of all the segments of the molecules are greater than 2 entanglements, the 'diluted' lengths of the inner generation segments are significantly smaller than one entanglement. However, the relaxation of the inner segments remain dominated by branch-

point friction and constraint release Rouse processes, and a description based on relaxation of entangled polymers provides a reasonable description for the stress relaxation of the current Cayley trees. The linear viscoelastic responses (lines in Figure 2) for both G3 and G4 are predicted satisfactorily. The predicted high-frequency regime (before the onset of entanglements) substantially deviates from the data, but this is typical problem and attributed both the tube-modeling (does not apply there) and experiments (segmental dynamics region approached) [47,51]. Relaxation of each generation introduces separate features in the linear relaxation (most easily seen in the phase angle). The predicted features are sharper than the experimental observations. This may be explained by the inevitable presence of slight polydispersity in molecular structure, which is not uncommon in complex model polymers [2,52] (see also section II.1 above). The experimental elastic modulus for G4 fails to reach the terminal slope at the lowest frequency probed. This likely reflects the presence of small fraction of side-products [19,32,36], as already discussed above (section II.1). An important remark concerns the actual relaxation which, based on BoB occurs well after the moduli crossover (due to relaxation of diluted inner segments), as seen clearly in Fig. 2. In fact, the predicted longest relaxation times are about 419 s and 1677 s for G3 and G4, respectively. These values differ sharply from the inverse G'-G'' crossover to the terminal region (33.3 and 200 s, as mentioned above). Given the lack of experimental data at low enough frequencies, we shall use below the terminal crossover as a measure of characteristic terminal time for extracting the Weissenberg number.

III.2. Transient uniaxial extension and shear: Data and modeling. In Figure 3, the transient data for G3 are depicted. The stress growth coefficient in Fig.3a exhibits strain hardening even at rates as low as $3x10^{-3}$ s^{-1}. This remarkable finding confirms the earlier results of van Ruymbeke et al. [19] . It is interesting to note that this lowest rate is below the terminal rate for G3 (around $2x10^{-2}$ rad/s, see Figure 2), and of course also below the estimated "bare" Rouse rates of the dendritic polymer (about 0.28 s^{-1}) or the outer branch (about 20 s^{-1}) [19]. In the former case, the bare Rouse time was considered as the time for the molecule to diffuse its own size with the friction given by monomer friction, and estimated as $\tau_R = r\ Z_{tot}^2\ \tau_e$ =3.6s, with Z_{tot} being the total molar mass divided by the entanglement molar mass and r is the radius of gyration contraction factor [32]. Note that the expected stretch relaxation time is much longer than this "bare" Rouse time, because the important stretch relaxation process is determined not from monomer friction, but from the friction of branch-point hopping. The calculation to obtain this longer stretch relaxation

time also is like a “Rouse calculation”, in which the monomer friction is replaced by branch point friction (and this is the route taken in BoB to calculate the stretch relaxation time). For the sake of clarity, in order to avoid confusing the two different Rouse times , we refer always to the Rouse time based on monomer friction as the “bare” Rouse time, whilst the longer relaxation time is called the “stretch relaxation time.” Viewed this way, the time is for the whole molecule and the dilution does not play any role. Concerning the outermost segments, their Rouse (or stretch) relaxation time is (star-like) $\tau_s=4Z_{seg}^2\ \tau_e$ = 0.05s, with Z_{seg} being the effective number of entanglements per segment. Further and more importantly, we can clearly observe in Fig.3a the steady state is reached at long enough times, hence Hencky strains (see also Figure 5 below). The unique relaxation data in this Figure were performed after stopping the extensional deformation at the same Hencky strain (ε_H = 3) for all strain rates investigated, before however steady state is attained. This will be further discussed below.

The respective shear data are depicted in Fig.3b. The transient shear viscosity exhibits well-known features of polymers [30]. In particular, it greatly depends on the imposed shear rate. At early times, the data collapse into the linear viscoelastic envelop, whereas later they depart. With increasing shear rate, a viscosity overshoot appears before a steady state value is reached, and becomes stronger at higher rates. The available data do not show any evidence of undershoot proceeding steady state. Moreover, there is no evidence of strain hardening in shear. The latter was reported for an entangled solution of multiply branched comb-like polystyrene, having long branches with about 10 entanglements each in the bulk, at Weissenberg numbers (based on terminal time) of $O(10^4)$, which were achieved by measuring at different temperatures [9]. The relaxation data (obtained by stopping the shear flow once the accumulated strain reached a value of about 20) suggest that viscosity relaxes faster in shear compared to uniaxial extension (Fig.3a), and this will be further discussed below.

Same remarks hold for the compiled elongational and shear data of Figure 4 for G4 (with the lowest imposed rate being 10^{-3} s^{-1}, and the accumulated strain being about 20 for the two lower and 25 for the two higher shear rates). Here, the bare Rouse time is estimated to be about 10.6 s. We note further, that the absolute values of stress growth coefficient are larger compared to G3, and this is expected since the structure of the latter consists of small number of segments between branches.

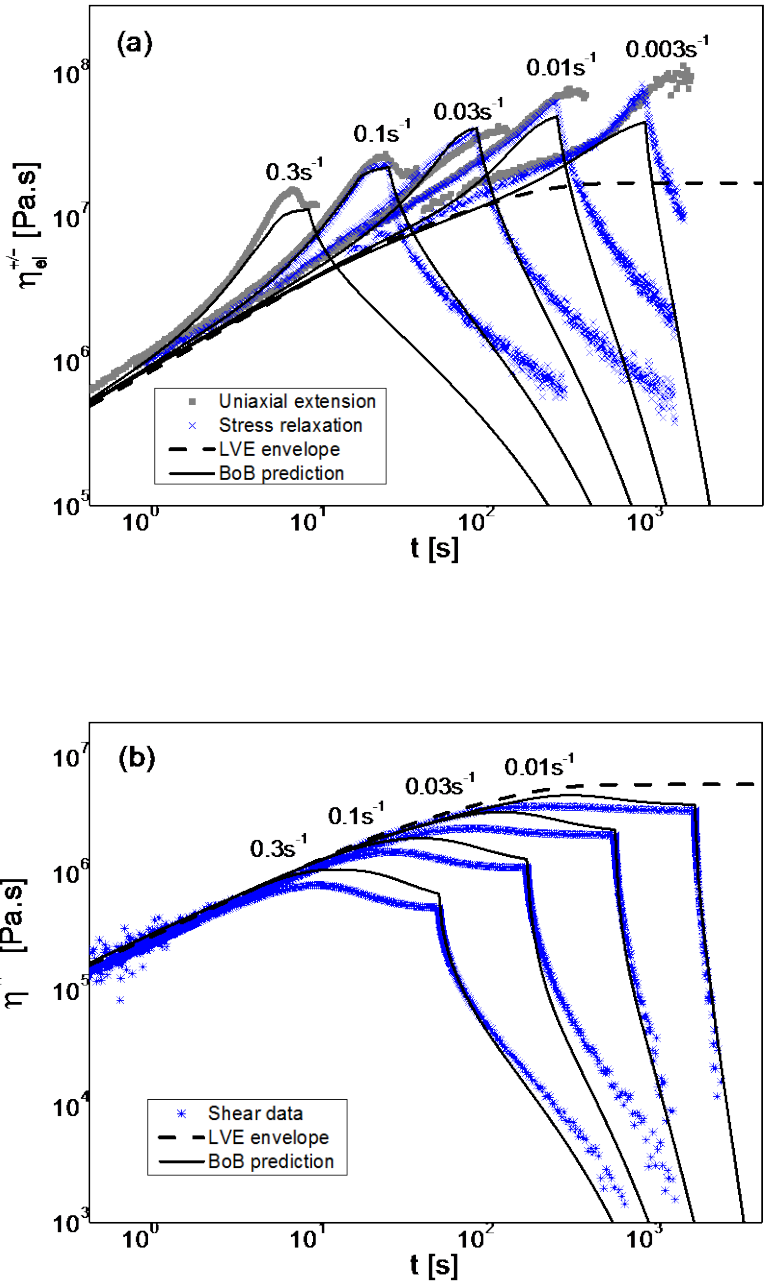

Figure 3: (a) Stress growth coefficient of G3 at different elongational rates (indicated in the plot) and its relaxation, at 180ºC. The gray data show the data from experiments performed up to steady state in uniaxial extension. The blue data show data on growth up of certain value (before steady state) and subsequent relaxation. The black dashed line is the LVE envelope (from Figure 2). (b) Respective start-up data in shear, indicating the time evolution of the transient viscosity (blue). The black dashed linear depicts the LVE

envelope. The viscosity relaxation data are recorded after steady state is attained and flow is subsequently stopped (see text). Black solid lines are predictions from BoB model.

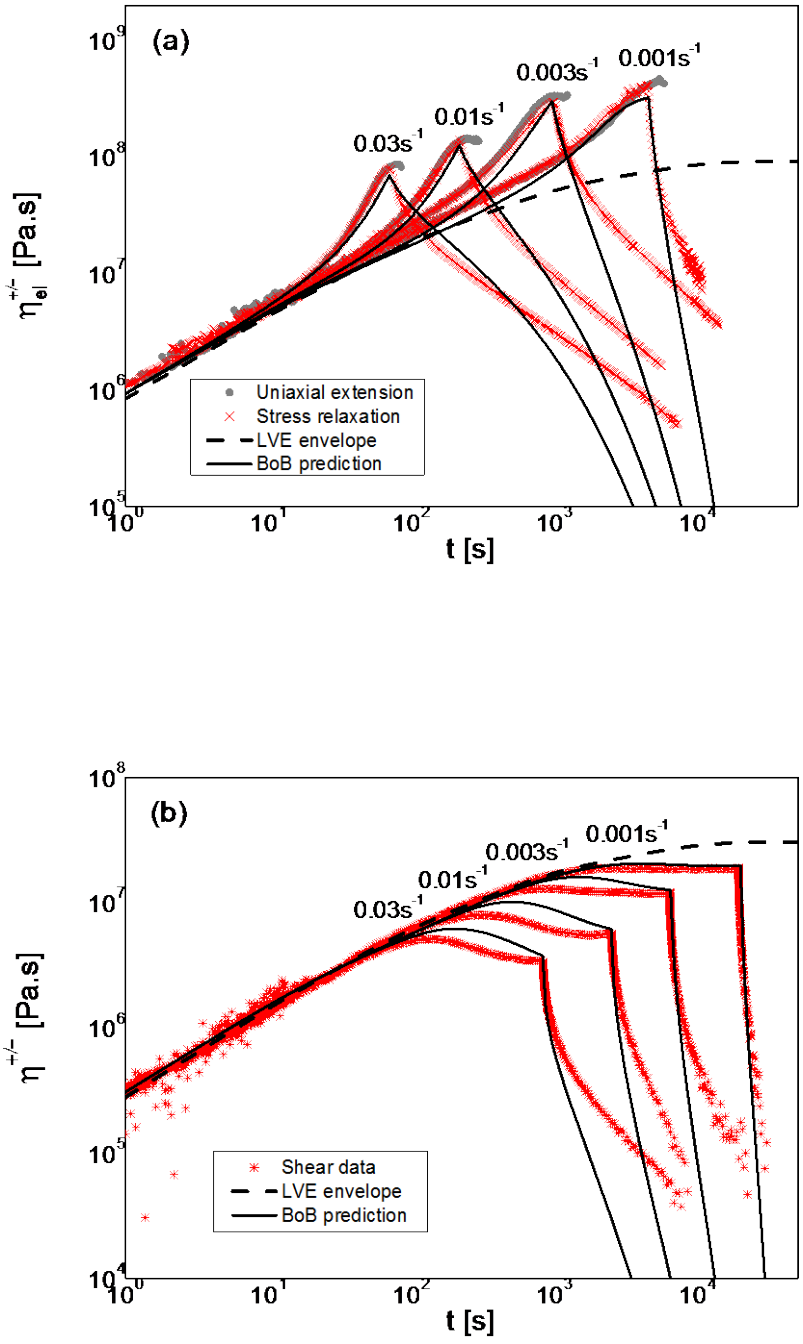

Figure 4: Respective data of Figure 3 for the transient response of G4 in uniaxial extension (a) and simple shear (b). The same temperature of 180ºC, rates and symbols are used, but different colors (here growth-relaxation cycle is depicted by red). Black solid lines are predictions from BoB model.

To predict the nonlinear flow behaviour, we aim to assign equivalent pom-pom modes [13] that describe the linear relaxation of the molecules and contain stretch and orientation relaxation times of the molecules (which are relevant to nonlinear flow properties). A pom-pom molecule is characterized by a modulus (g), the maximum stretch that the backbone can support before branch points starts withdrawing in the backbone tube (q, also the number of side arms in each side of the backbone for a symmetric pom-pom molecule), the stretch relaxation time (τ_s), and the orientation relaxation time (τ_o). In the differential version of the pom-pom model, the pre-averaged stretch λ satisfies the following equation [5,44]

$$\frac{d\lambda}{dt} = \lambda\,\mathbf{K} : \mathbf{S^T} - \frac{(\lambda-1)}{\tau_s}\exp\left[\frac{2}{q-1}(\lambda-1)\right]. \quad (3)$$

Here, **K** and **S** are the deformation rate and the pre-averaged backbone orientation tensor, respectively. The evolution of the orientation tensor is conveniently described by the auxiliary tensor **A** with $\mathbf{S} \equiv \frac{\mathbf{A}}{\mathrm{tr}(\mathbf{A})}$ and satisfying equation (4):

$$\frac{d\mathbf{A}}{dt} = \mathbf{K}.\mathbf{A} + \mathbf{A}.\mathbf{K^T} - \frac{1}{\tau_o}(\mathbf{A}-\mathbf{1}). \quad (4)$$

The stress evolution is given by the following equation:

$$\boldsymbol{\sigma} = 3\,g\,\lambda^2(t)\mathbf{S}(t). \quad (5)$$

The advantage of using the set of evolution equations (3)-(5) is that, for both uniaxial and shear start-up the evolution of **A** and hence the orientation tensor **S** can be solved analytically. On the other hand, the evolution of the stretch is solved numerically. In a multimode pom-pom description, a set of such pom-pom molecules is considered, and the stress is calculated by a simple sum over stress from each of the pom-pom modes. The numerical calculation for the linear rheology prediction offers a natural choice to resolve the molecules in terms of multiple *independent* pom-pom modes [8,40]: the parts of the molecules relaxing at a certain time t_c have orientation relaxation time $\tau_o = t_c$; the time at which these parts (segments) can move coherently with the chain ends define the stretch relaxation time τ_s. In addition, the branching topology from the currently relaxing segments define the maximum stretch q as the priority variables [53], and the modulus

relaxed in this time interval sets the modulus of the pom-pom mode. Based on the pom-pom model [13], equating the maximum tension with the tension along the backbone gives a maximum stretch of q. In the present case of Cayley tree, we consider any molecular segment between two branch points being equivalent to an effective the backbone in pom-pom molecule. At each time interval, separate pom-pom modes are used to describe relaxation due to chain escape from the confining tube and due to the constraint release on the chains still confined in the tube potential at this time.

When the flow rate is much slower than the stretch relaxation time, the geometric criteria for assigning the maximum stretch lead to an over-prediction of the extensional hardening for randomly branched polymers, hence flow-dependent modifications of the priority variables are required in order to describe the experimental data [8,40]. However, the available approximation for this flow modification requires vastly different relaxation times (as in industrial randomly branched low density polyethylene) and is not valid for symmetric model polymers. Fortunately, at the flow rates considered, the bare priority is found to describe the amount of extension hardening reasonably well for the two dendritically branched polymers considered here.

When the flow is stopped, the stress evolution from equation (5) is asymptotically equivalent to:

$$\frac{d\mathbf{S}}{dt} = -\frac{1}{\mathrm{B}\,\tau_o}\left(\mathbf{S} - \frac{\mathbf{1}}{3}\right) \qquad (6)$$

with $\mathrm{B} = \mathrm{tr}(\mathbf{A})$ [54,55]. The trace of the auxiliary tensor has no physical significance and can become arbitrarily large. We chose to work with the tensor A during the start-up flow, and construct the orientation tensor S at the start of the cessation of the flow. Subsequent relaxation in the absence of flow is calculated from equation 6 with the choice $\mathrm{B} = 1$. Other commonly used variant of stress evolution equations considers $\mathrm{B} = \lambda^2$ [54] that couples the orientation and the stretch evolution together and requires both of these to be solved simultaneously numerically. The origin of such a coupling can be rationalized by considering the increase in the reptation time of the pom-pom backbone in the stretched backbone tube in the absence of constraint release. Since our pom-pom modes describe relaxation of different parts of a dendritic molecule, if such orientation-stretch coupling is important, its form should be different from $\mathrm{B} = \lambda^2$. Here, the choice of $\mathrm{B} = \lambda^2$ does not

affect the approach to steady state and predicts only marginally higher steady state stress. The stress decay, especially at high rates, is delayed significantly compared to the experiments (and compared to the B=1 choice used here).

The solid lines in Figures 3 and 4 depict the predicted uniaxial stress growth/decay coefficients for G3 and G4, respectively. Except for the lowest flow rate for G3, the stress growth coefficient for uniaxial extension is described reasonably well without any adjustable parameter. The initial relaxation after uniaxial relaxation is also described well. But eventually, in all cases, the experimental relaxation becomes much slower than predicted. The experimental long-time relaxation is approximately power-law decay (linear in log-log plot). Such a non-exponential behaviour may reflect coupling between different modes (see also discussion on the parameter B above): the stretches in different segments of the dendritic macromolecule are coupled, hence describing them as relaxing independently is not completely correct [15,44]. Once stretched, the stretch of inner segments can only relax once the stretches in the outer segments had already relaxed. This sets a formidable challenge for future work. We further note that the start-up shear predictions (in Figures 3b and 4b) show significant overshoots absent in the experimental data. The physical origin of such overshoot in the pom-pom model is due to stretching of the tubes as they start orienting along the flow. We conjecture that the short segments in the experimental system prohibit such stretch and stress overshoot. The steady state shear stress is described reasonably well. The stress relaxation after shear cessation is described well except for the high rates for G4, but as already mentioned, there is a possibility of structural polydispersity in the dendritic polymers, which can affect flow properties in different ways.

III.3. Compilation of data and scaling. A phenomenological analysis of the evolution of material functions in uniaxial extension and shear is presented in Figure 5. A measure of the level of strain hardening achieved can be obtained by the strain hardening factor, which is defined as the ratio of the stress growth coefficient $\eta_{el}^{+}(t,\dot{\varepsilon})$ to the respective LVE value, $\mathrm{SHF} = \eta_{el}^{+}(t,\dot{\varepsilon}) / \eta_{LVE}^{+}(t)$ and is plotted in Figure 5(a) for the different values of strain rates used for G3 and G4. The onset of strain hardening is marked by the departure of SHF from 1. The stronger hardening of G4 compared to G3 at the same stretch rate is evident. On the other hand, focusing on the G3 data, there is an unambiguous non-monotonic dependence

of SHF and in particular its peak value on stretch rate. First, we note that at rates $\dot{\varepsilon} \geq 0.03$ s^{-1}, i.e. above the terminal moduli crossover where the segments are not fully relaxed (Fig. 2), the SHF is expectedly enhanced with increasing rate. On the other hand, as the stretch rate decreases below its terminal value, an increase of SHF is observed. The latter is a consequence of the definition of the SHF and the shape of the LVE envelope. Eventually, at lower rates SHF will drop to 1, at the linear envelope. The (fewer) data with G4 are consistent with this picture. The important message is that these dendritically branched polymers strain harden significantly even when stretched at rates below their terminal rate, in sharp contrast to linear or star polymers [56]. Furthermore, in Figure 5(b) we plot the fractional overshoot in shear viscosity $\eta^+(t,\dot{\gamma})_{max} / \eta^+(\dot{\gamma})_{steady}$ against Wi_D, for G3 and G4. Wi_D is the Weissenberg number based on a characteristic time τ_D, extracted from the inverse moduli crossover frequency as discussed above), $Wi_D = \dot{\gamma}\tau_D$. The viscosity overshoot is a measure of maximum shear deformation of the dendritic polymers at steady state. For comparison we include in this figure data from the literature [30] with linear polystyrene of molar mass 185k (about 14 entanglements). First, we note that at low rates (up to about Wi_D=1) there is no overshoot (see also Figures 3b and 4b). We further observe that the data for both G3 and G4 are very close, almost collapse (given the experimental uncertainties) and exhibit a different (stronger) dependence on Wi_D compared to entangled linear polymers (which exhibit a power-law with exponent 0.25). However, the available dendritic data are not enough in order to extract a reliable power-law exponent. The value of shear strain at the viscosity overshoot is plotted against Wi_D for G3, G4 and the linear polystyrene in Figure 5(c). First, at low Wi_D the data are constant, indicating a saturation of peak strain (which is the maximum instantaneous shear deformation). For linear polymers this value is 2.3 and known to reflect segmental orientation as predicted by the tube model. For comb polymers this value is also about 2.3 as reported by Snijkers et al. [37]. For the dendritic Cayley trees here, the available experimental data suggest a value of 2.6 (Figure 5(c)). Further, with increasing Wi_D the peak strain increases, reflecting stronger deformation (stretching). It follows a power-law with exponent of 0.33 for linear polymers and much smaller (0.1) for both dendritics. This result reflects the molecular structure which makes it more difficult to deform a Cayley-tree (more) compact structure compared to a linear flexible polymer.

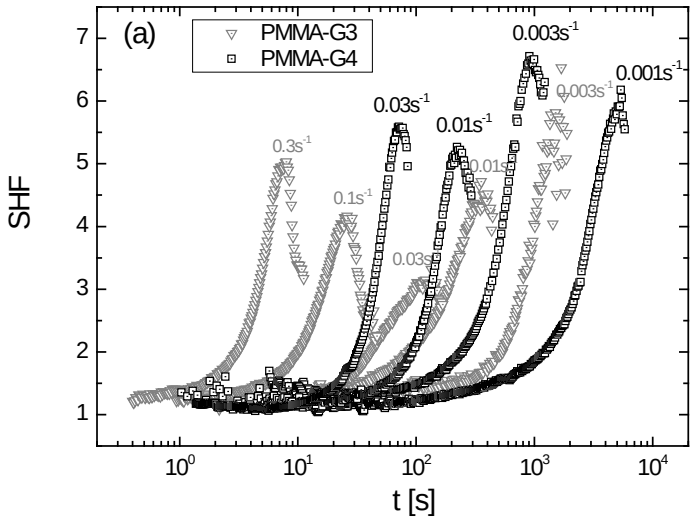
(a)
PMMA-G3
PMMA-G4
SHF
t [s]
0.3s-1
0.1s-1
0.03s-1
0.01s-1
0.003s-1
0.001s-1

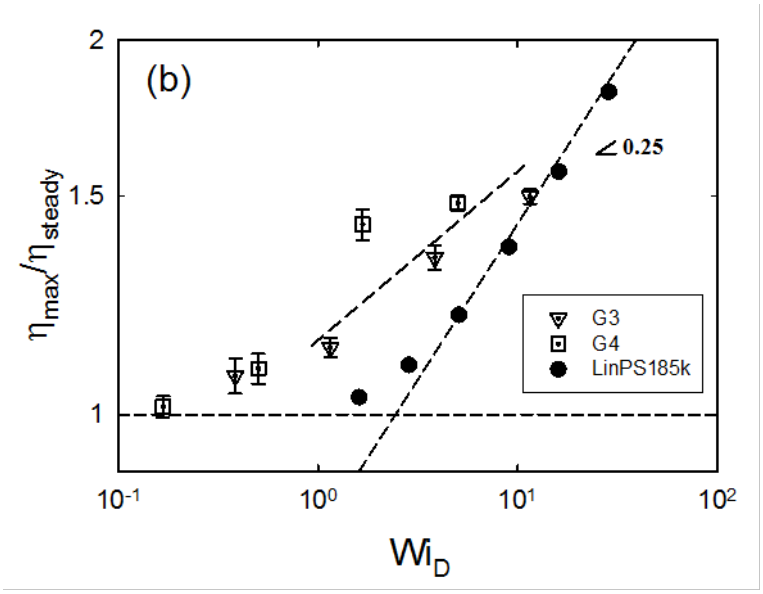
(b)
G3
G4
LinPS185k
∠ 0.25
ηmax/ηsteady
WiD

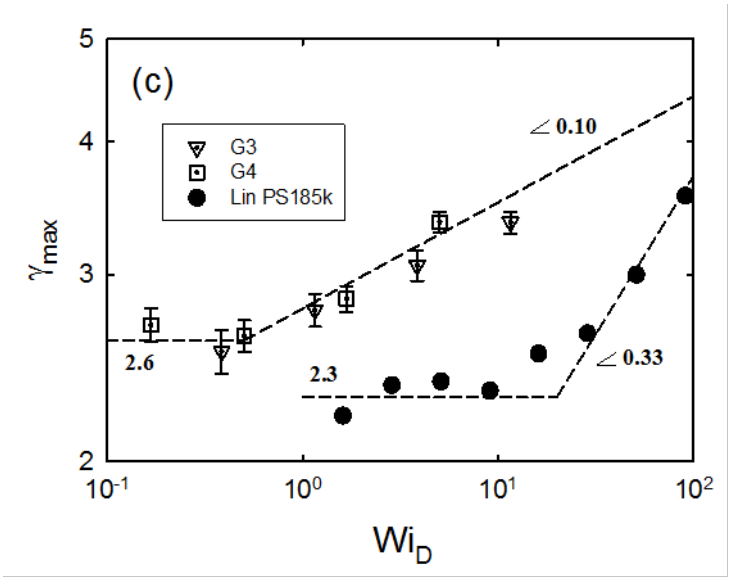
(c)
G3
G4
Lin PS185k
∠ 0.10
∠ 0.33
2.6
2.3
γmax
WiD

Figure 5: (a) Ratio of the stress growth coefficient to the respective LVE value at different stretch rate for G3 (gray) and G4 (black) (b) Normalized peak viscosity and (c) peak strain at the maximum viscosity as functions of the Weissenberg number based on the inverse terminal G'G'' crossover (see text). In (b) and (c) we show for comparison data with linear polystyrene LinPS185k, whereas the lines are drawn to guide the eye (see text).

Since the issue of steady state is one of the challenges, we elucidate this further in Figure 6 below, where the tensile stress for both G3 and G4 is plotted against the Hencky strain for the different values of Hencky strain rate tested (in Figures 3 and 4). Indeed, this figure demonstrates the attendance of steady state for both polymers. Steady state is reached at lower values of Hencky strain for larger Hencky strain rates. Moreover, for the two larger rates of G3 one may note the appearance of a broad overshoot. Such overshoot has been reported for branched polymers [19] but here the limited data do not allow further discussion. Understanding the extensional overshoot remains a challenge in the field, however the present polymers are not amenable to the currently available experimental window.

The steady state extensional and shear viscosities are plotted together versus the respective Hencky strain and shear rates in Figure 7, along with the dynamic viscosity data (versus oscillatory frequency. The latter are multiplied by 3 (Trouton ratio). It is noted that the empirical Cox-Merz rule validated for this class of hyperbranched polymers. This is not expected to a first sight since branching contributes to deviations from this rule [57], however we note that the branches are barely entangled and this may be at the origin of the good agreement of dynamic and steady shear data. Moreover, both shear/dynamic and extensional data exhibit thinning with increased rates. In the former case, the shear data follow a scaling law with thinning slope of -0.7 for both generations, which is smaller than the usual slope of about -0.82 which has been reported for entangled linear polymers [30,16]. On the other hand, the extensional data exhibit a thinning slope of -0.5, again for both G3 and G4, with the latter having higher values (see also Figures 3 and 4). This complies with the BoB predictions and further confirms earlier findings with linear or pom-pom polymers [10] and is explained in the context of tube modeling [58]. Finally, the shear/dynamic data are always below the respective extensional data, due to strain hardening in this range of rates (see Figures 3 and 5a). Furthermore, we remark that the extensional data do not show a tendency to overlap the dynamic and shear data at low rates,

as is normally expected. However, it is reported that for branched polymers the steady viscosity in uniaxial extension is constant at low stretch rate (overlaps with $3\eta^*$), then it exhibits extension thickening and after an overshoot it thins at higher rates [59]. Based on this, we conjecture that the data of Figure 7 are in the thinning regime past but close to the peak, and they are above the level of the zero-rate viscosity (not reached) which is expected to coincide with the zero-shear dynamic and shear viscosities, accounting for the Trouton ratio.

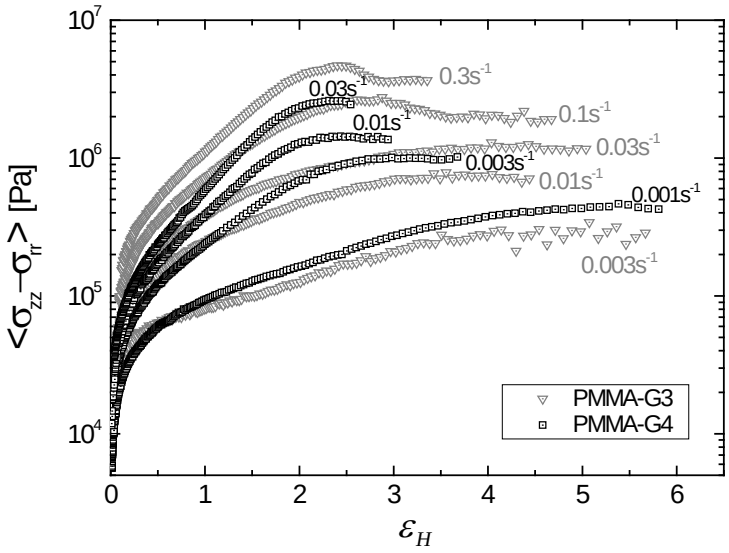

Figure 6: Net tensile stress for G3 (gray) and G4 (black) versus Hencky strain for different values of the imposed Hencky strain rate, at 180ºC.

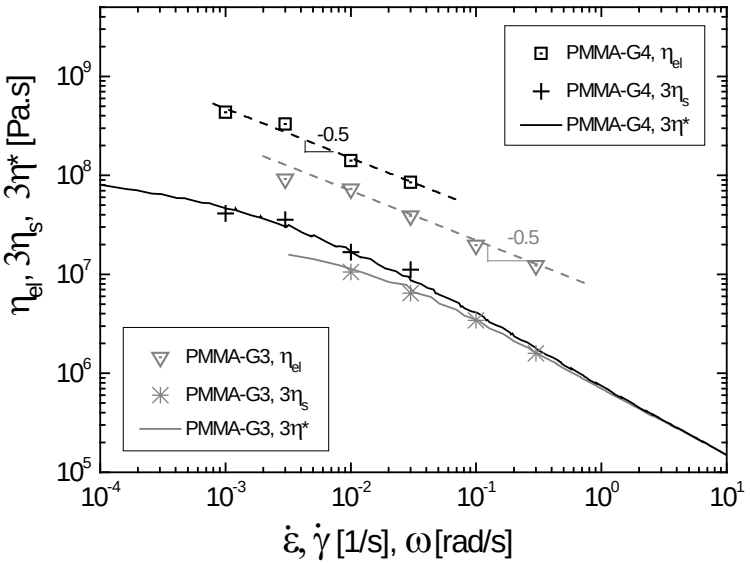

Figure 7: Steady-state data on extensional viscosity (open symbols), shear viscosity (crosses and stars) and dynamic complex viscosity (solid lines, multiplied by the Trouton ratio 3) plotted against Hencky strain rate, shear rate and oscillatory frequency, respectively, on the same axis. Data are shown for G3 (gray) and G4 (black). The dashed lines through the extensional data have a slope of -0.5.

III.4. Stress relaxation upon flow cessation. Figure 8 reports the stress relaxation data upon cessation of shear or extensional flow, for the two dendritic PMMAs, G3 (a) and G4 (b). In the latter case, stress relaxation was recorded after cessation of steady shear flow. In the former case, the extensional flow was arrested before (albeit close to) the steady state and at nearly the same deformation in terms of Hencky strain (values reported in the caption). In the same figure we plot the relaxation modulus G(t) extracted from the linear viscoelastic data of Figure 2. Finally, four dashed vertical lines are plotted, representing the characteristic Rouse time of an effective outer branch (arm) ($\tau_{R_{Arm}}$) and the whole dendrimer ($\tau_{R_{Bare}}$), as well as the characteristic terminal times extracted from the low-frequency crossover ($\tau_{D_{CO}}$) and from BoB modelling ($\tau_{D_{BoB}}$). These times are discussed in section III.1 above. We observe that the nonlinear stress relaxations in shear and extension are very different from the linear relaxation. In shear, for a wide range of times, up to about 1 s, the stress is almost constant (this is more evident in Figure 9 below due to different scale). Subsequently, relaxation becomes more pronounced, and beyond $\tau_{D_{BoB}}$ the

stress for both G3 and G4 becomes essentially independent of the rate (i.e., the material loses its memory) and relaxes by linear mechanism as G(t). Indeed, one expects that after nonlinear deformation polymer reorganizes and relaxes thermally according to its G(t) in the end. The situation is different for the extensional data. Similarly to the shear case, the net tensile stress relaxation data remain distinct for different stretch rates at short times, suggesting that the nonlinear induced state of the material has not relaxed during the experiment, whereas they virtually collapse (especially for G3) at longer times above $\tau_{D_{BoB}}$. Remarkably, even if at these times the polymeric response is linear, it is evident from both Figures 8(a) and 8(b) that complete relaxation of this stress is slower than G(t). This suggests the strong effects of initial extensional deformation, even at very low stretch rates. Note in particular, that the two lowest rates used with G4 (10^{-3} and $3x10^{-3}$ s^{-1}) are below the Rouse rate of the outer segment, yet strong strain hardening is observed (Figure 4) and strong nonlinear effects dominate the subsequent relaxation. It is evident that the extensional relaxation is much broader than the respective linear and nonlinear shear, and as a consequence the extensional stress will relax well after complete relaxation of G(t). As already noted above in conjunction with the description of the data of Figs. 3 and 4, this interesting effect should reflect the coupling of stretch in different parts (generations) of the dendritic macromolecule, and is of course much more significant in extensional deformation, in the examined parameter range. As a result of this coupling, the stress relaxation upon cessation of uniaxial extensional flow is expected to be substantially delayed. For completeness, we note that a similar behavior was reported recently for bidisperse blends of long and short linear polystyrenes undergoing relaxation after uniaxial extension was stopped [26]. In particular, for a blend of 50% short (7 entanglements) -50% long (41 entanglements) linear polystyrene chains, the elongational stress relaxation exhibited power-law with an exponent of about -1 and appeared slower than that of either component. This was attributed to the remaining, persistent flow induced orientation of initially retracted long chains in a sea of relaxed short chains. The analogy with the present work is that the induced orientation can be considered as coupling of stretch in different chains. Concerning the present data, given the small range of times we refrain from considering power laws. Unfortunately, we do not have independent information of the flow-induced stretching in different generations and respective relaxation upon flow cessation (in fact, very limited data exist in general [7,12,60]) since this requires deuterated samples which are not available currently.

To further elucidate the different relaxation after shear and extensional flow, we represent the data of Figure 8 in normalized form in Figure 9. In particular, the decreasing transient stresses $\bar{\eta}_{el}(t)$ for extension or $\bar{\sigma}(t)$ for shear, are normalized by the corresponding values of extensional stress growth coefficient when extensional flow was stopped (at almost the same value of Hencky strain ε_H=3 for G3 and steady stress for G4) or shear stress at steady state (albeit at constant shear strain of 20). The broader and slower relaxation of extensional stress compared to shear stress is unambiguous for both G3 (a) and G4 (b). We note further that elongational flow (with zero vorticity tensor) deforms the polymer more severely than shear, despite the lower strain. Concomitantly, the viscosity is much higher in the former case due to hardening (Figure 7). Concerning G4 (Figure 9b), the relaxation is slower compared to G3 (Figure 9a) and again the broader relaxation in extension as opposed to shear is evident. Although the data can be agreed in this context, for quantitative analysis further work will be required in the future, especially accounting for the coupling of stretches as mentioned above.

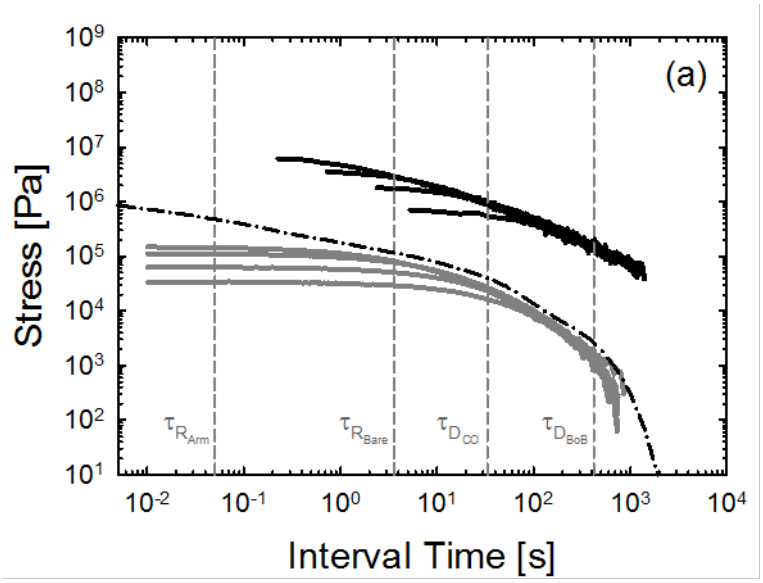

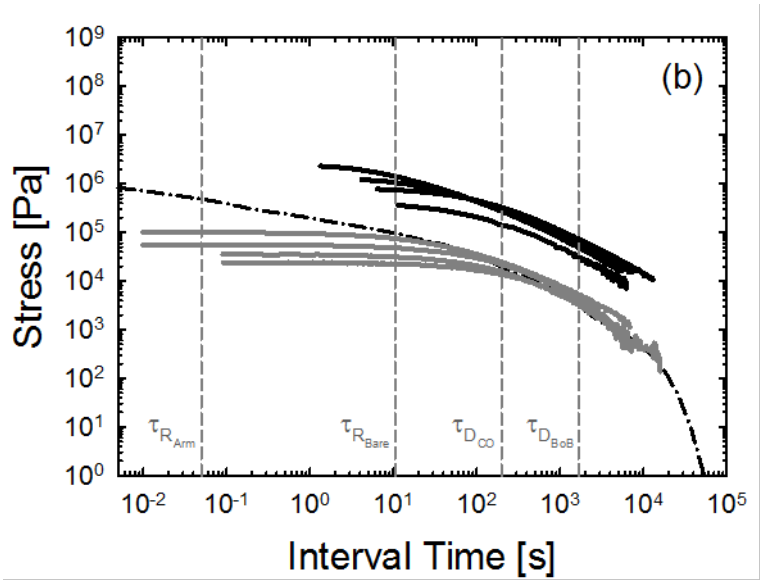

Figure 8: Stress relaxation of G3 (a) and G4 (b) as a function of time after flow cessation. Interval time is the difference between the absolute time and the time when relaxation starts. Black curves depict the relaxation of G3 (a) and G4 (b) after extension, respectively. Gray curves show the relaxation of after shear in both cases. The applied rates and accumulated strain at cessation of flow are: (a) for shear, from top to bottom at short times 0.3, 0.1, 0.03, 0.01 s^{-1} (20 strain units for each shear rate); for extension, from top to bottom: 0.1, 0.03, 0.01, 0.003 s^{-1} (3 strain units for each extension rate). (b) for shear, from top to bottom at short times 0.03, 0.01, 0.003, 0.001 s^{-1} (25 strain units for each shear rate); for extension, from top to bottom 0.03,0.01,0.003,0.001 s^{-1} (corresponding strain units: 2.1, 2.2, 3, 4.5, respectively). The relaxation modulus curve of the respective dendritic polymer is reported in both figures as a reference (dash-dot line). The characteristic Rouse times of the outer branch ($\tau_{R_{Arm}}$) and the whole molecule ($\tau_{R_{Bare}}$), as well as the characteristic terminal times from the low-frequency crossover ($\tau_{D_{CO}}$) and from BoB modelling ($\tau_{D_{BoB}}$) are reported as reference (see text).

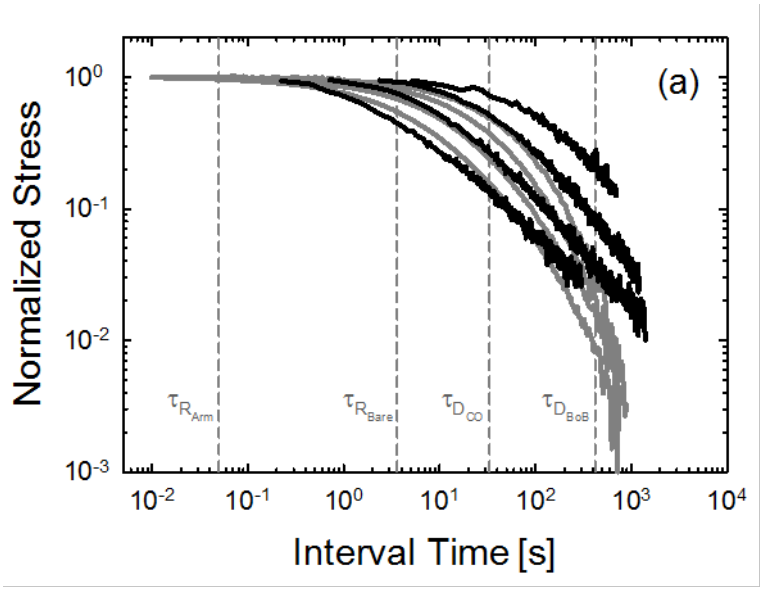

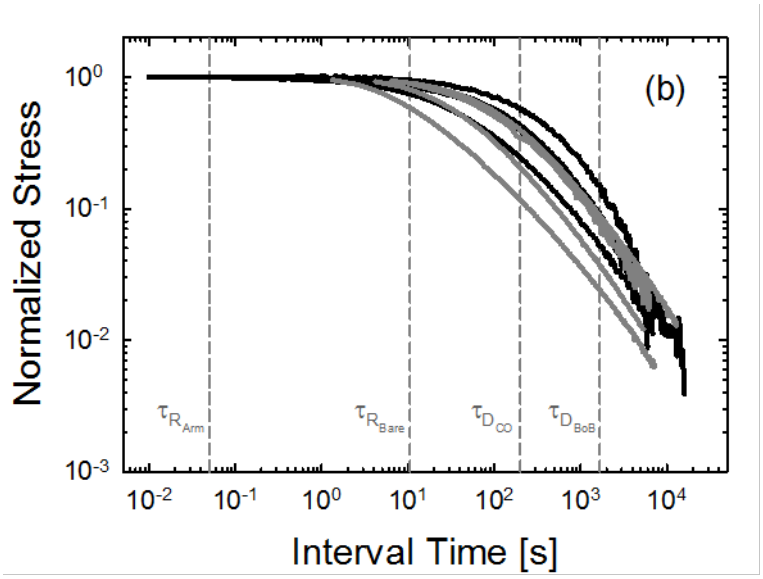

Figure 9: Data of Figure 8 normalized by the respective values of shear stress or stress growth coefficient when shear or extensional flow was stopped (see text). Characteristic times are reported for reference as in figure 8.

IV. Concluding remarks

We have investigated the growth, steady state and subsequent relaxation of viscosity during uniaxial extensional and shear deformation of model, well-characterized Caley-tree PMMA structures of third and fourth generation, having short, equal branches (about 2.4 entanglements each). The experimental data were obtained with state of the art instrumentation (FSR and CPP). The extension and shear rates cover a range extending from LVE terminal relaxation to rubbery regime. Despite the small values of the imposed rates, significant strain hardening was observed. At the same time, viscosity overshoots signaled the deformation of these polymers in shear as well. Extensional relaxation is broader and slower than in shear. The latter is different from that of the linear stress (or relaxation modulus G(t)) but at long times it appears to approach it. The unusual relaxation of viscosity upon cessation of uniaxial extensional is consistent with a stronger deformation in extension and the related strain hardening. The BoB framework based on independent pom-pom modes describes the experimental data in linear and nonlinear shear (growth and relaxation) and extension (growth and initial relaxation) reasonably well and without fit parameters. This is remarkable, considering the fact that a segment between two branches in these molecules is less than 3 entanglements long. The slow relaxation upon cessation

of extensional flow may reflect coupling of the stretches in different generations. To describe it the pom-pom modes cannot be considered as independent, hence a modified model should be considered. Whereas this calls for further investigations, it shows a way to use strong flows for tailoring properties of polymeric materials and effectively enhancing their 'elastic memory'. Furthermore, there is unambiguous evidence of steady state in extension. The small molar mass of branches appears to be responsible for the validation of the empirical Cox-Merz rule. At the same time the high-rate regime in extension follows a thinning slope of -0.5 in accordance with predictions and findings with linear and branched polymers. This power-law is virtually followed by the shear data as well.

In general, at first sight it is a surprise that BoB does such a good job in predicting the linear and nonlinear viscoelasticity of such a polymer with barely entangled branches. We attribute this to the difference in the strength of the entanglement constraints at the branch point as opposed to the respective linear entangled polymers. This ensures that the dynamics of the inner segments remain dominated by the branch-point friction instead of the monomer friction and a framework based on well-entangled polymers continue to capture the relaxation of unentangled (in the dilated tube) inner segments. Actually, the present case may be thought as a limit of validity of the BoB model.

It is hoped that the present unique data set can motivate further developments in modeling by testing the above stretch coupling idea and predicting viscosity relaxation consistently in shear and extension and eventually advancing constitutive modeling. At the same time, measurements of polymer conformation in-situ or ex-situ (via quenching below glass temperature) and attempts the probe nonlinear material functions (including normal stresses) at higher rates will further advance the field.

Acknowledgments

We are grateful to Professor Akira Hirao (Tokyo Institute of Technology) for generously providing the polymers used in this work. Partial support by EU under the People Programme (Marie Sklodowska-Curie Actions, FP7/2007-2013, Supolen, REA grant 607937) and the Aage og Johanne Louis-Hansen Foundation is gratefully acknowledged. DV thanks Ole Hassager for hosting him at the Danish Polymer Center in spring 2016.

References

[1] Snijkers, F., R. Pasquino, P. D. Olmsted, and D. Vlassopoulos, “Perspectives on the Viscoelasticity and Flow Behavior of Entangled Linear and Branched Polymers,” J. Phys. Condens. Matter **27**, 1–25 (2015).

[2] van Ruymbeke, E., H. Lee, T. Chang, a Nikopoulou, N. Hadjichristidis, F. Snijkers, and D. Vlassopoulos, “Molecular Rheology of Branched Polymers: Decoding and Exploring the Role of Architectural Dispersity through a Synergy of Anionic Synthesis, Interaction Chromatography, Rheometry and Modeling.,” Soft Matter **10**, 4762–77 (2014).

[3] Li, S. W., H. E. Park, J. M. Dealy, M. Maric, H. Lee, K. Im, H. Choi, T. Chang, M. S. Rahman, and J. Mays, “Detecting Structural Polydispersity in Branched Polybutadienes,” Macromolecules **44**, 208–214 (2011).

[4] Torres, E., S.-W. Li, S. Costeux, and J. M. Dealy, “Branching Structure and Strain Hardening of Branched Metallocene Polyethylenes,” J. Rheol. **59**, 1151–1172 (2015).

[5] McLeish, T. C. B., J. Allgaier, D. K. Bick, G. Bishko, P. Biswas, R. Blackwell, B. Blottie, N. Clarke, B. Gibbs, D. J. Groves, A. Hakiki, R. K. Heenan, J. M. Johnson, R. Kant, D. J. Read, and R. N. Young, “Dynamics of Entangled H-Polymers : Theory , Rheology , and Neutron-Scattering,” Macromolecules **32**, 6734–6758 (1999).

[6] McLeish, T. C. B., “Tube Theory of Entangled Polymer Dynamics,” Adv. Phys. **51**, 1379–1527 (2002).

[7] McLeish, T. C. B., N. Clarke, E. de Luca, L. R. Hutchings, R. S. Graham, T. Gough, I. Grillo, C. M. Fernyhough, and P. Chambon, “Neutron Flow-Mapping: Multiscale Modelling Opens a New Experimental Window,” Soft Matter **5**, 4426–4432 (2009).

[8] Read, D. J., D. Auhl, D. Chinmay, J. den Doelder, M. Kapnistos, I. Vittorias, and T. C. B. McLeish, “Linking Models of Polymerization and Dynamics to Predict Branched Polymer Structure and Flow,” Science (80-.). **333**, 1871–1874 (2011).

[9] Liu, G., S. Cheng, H. Lee, H. Ma, H. Xu, T. Chang, R. P. Quirk, and S. Q. Wang, “Strain Hardening in Startup Shear of Long-Chain Branched Polymer Solutions,” Phys. Rev. Lett. **111**, 8–11 (2013).

[10] Nielsen, J. K., H. K. Rasmussen, M. Denberg, K. Almdal, and O. Hassager, “Nonlinear Branch-Point Dynamics of Multiarm Polystyrene,” Macromolecules **39**, 8844–8853 (2006).

[11] Tezel, A. K., L. G. Leal, J. P. Oberhauser, R. S. Graham, K. Jagannathan, and T. C. B. McLeish, “The Nonlinear Response of Entangled Star Polymers to Startup of Shear Flow.,” **1193**, 1193–1214 (2009).

[12] Ruocco, N., L. Dahbi, P. Driva, N. Hadjichristidis, J. Allgaier, A. Radulescu, M. Sharp, P. Lindner, E. Straube, W. Pyckhout-Hintzen, and D. Richter, “Microscopic Relaxation Processes in Branched-Linear Polymer Blends by Rheo-SANS,” Macromolecules **46**, 9122–9133 (2013).

[13] McLeish, T. C. B. and R. G. Larson, “Molecular Constitutive Equations for a Class of Branched Polymers: The Pom-Pom Polymer,” J. Rheol. **42**, 81 (1998).

[14] Lentzakis, H., D. Vlassopoulos, D. J. Read, H. Lee, T. Chang, P. Driva, and N. Hadjichristidis, “Uniaxial Extensional Rheology of Well-Characterized Comb Polymers,” J. Rheol. **57**, 605 (2013).

[15] Lentzakis, H., C. Das, D. Vlassopoulos, and D. J. Read, “Pom-Pom-like Constitutive Equations for Comb Polymers,” J. Rheol. **58**, 1855–1875 (2014).

[16] Wingstrand, S. L., N. J. Alvarez, Q. Huang, and O. Hassager, “Linear and Nonlinear

Universality in the Rheology of Polymer Melts and Solutions," Phys. Rev. Lett. **115**, 78302 (2015).
[17] Marrucci, G. and G. Ianniruberto, "Interchain Pressure Effect in Extensional Flows of Entangled Polymer Melts," Macromolecules **37**, 3934–3942 (2004).
[18] Wagner, M. H. and V. H. Rolón-Garrido, "Verification of Branch Point Withdrawal in Elongational Flow of Pom-Pom Polystyrene Melt," AIP Conf. Proc. **1027**, 412–414 (2008).
[19] van Ruymbeke, E., E. B. Muliawan, S. G. Hatzikiriakos, T. Watanabe, a. Hirao, and D. Vlassopoulos, "Viscoelasticity and Extensional Rheology of Model Cayley-Tree Polymers of Different Generations," J. Rheol. **54**, 643 (2010).
[20] Ruymbeke, E. Van, J. Nielsen, and O. Hassager, "Linear and Nonlinear Viscoelastic Properties of Bidisperse Linear Polymers : Mixing Law and Tube Pressure Effect," J. Rheo **54**, 1155–1172 (2010).
[21] Ianniruberto, G., A. Brasiello, and G. Marrucci, "Simulations of Fast Shear Flows of PS Oligomers Confirm Monomeric Friction Reduction in Fast Elongational Flows of Monodisperse PS Melts as Indicated by Rheooptical Data," Macromolecules **45**, 8058–8066 (2012).
[22] Yaoita, T., T. Isaki, Y. Masubuchi, H. Watanabe, G. Ianniruberto, and G. Marrucci, "Primitive Chain Network Simulation of Elongational Flows of Entangled Linear Chains: Stretch/orientation-Induced Reduction of Monomeric Friction," Macromolecules **45**, 2773–2782 (2012).
[23] Ianniruberto, G., "Extensional Flows of Solutions of Entangled Polymers Confirm Reduction of Friction Coefficient," Macromolecules **48**, 6306–6312 (2015).
[24] Das, C., N. J. Inkson, D. J. Read, M. a. Kelmanson, and T. C. B. McLeish, "Computational Linear Rheology of General Branch-on-Branch Polymers," J. Rheol. **50**, 207 (2006).
[25] Nielsen, J. K., H. K. Rasmussen, and O. Hassager, "Stress Relaxation of Narrow Molar Mass Distribution Polystyrene Following Uniaxial Extension," J. Rheol. **52**, 885 (2008).
[26] Hengeller, L., Q. Huang, A. Dorokhin, N. J. Alvarez, K. Almdal, and O. Hassager, "Stress Relaxation of Bi-Disperse Polystyrene Melts," Rheol. Acta **55**, 303–314 (2016).
[27] Bach, A., H. K. Rasmussen, and O. Hassager, "Extensional Viscosity for Polymer Melts Measured in the Filament Stretching Rheometer," J. Rheol. **47**, 429 (2003).
[28] Schweizer, T. and W. Schmidheiny, "A Cone-Partitioned Plate Rheometer Cell with Three Partitions (CPP3) to Determine Shear Stress and Both Normal Stress Differences for Small Quantities of Polymeric Fluids," J. Rheol. **57**, 841 (2013).
[29] Snijkers, F. and D. Vlassopoulos, "Cone-Partitioned-Plate Geometry for the ARES Rheometer with Temperature Control," J. Rheol. **55**, 1167 (2011).
[30] Costanzo, S., Q. Huang, G. Ianniruberto, G. Marrucci, O. Hassager, and D. Vlassopoulos, "Shear and Extensional Rheology of Polystyrene Melts and Solutions with the Same Number of Entanglements," Macromolecules **49**, 3925–3935 (2016).
[31] Van Ruymbeke, E., K. Orfanou, M. Kapinstos, H. Iatrou, M. Pitsikalis, N. Hadjichristidis, D. J. Lohse, and D. Vlassopoulos, "Entangled Dendritic Polymers and beyond: Rheology of Symmetric Cayley-Tree Polymers and Macromolecular Self-Assemblies," Macromolecules **40**, 5941–5952 (2007).
[32] Hirao, A. and A. Matsuo, "Synthesis of Chain-End-Functionalized Poly(methyl Methacrylate)s with a Definite Number of Benzyl Bromide Moieties and Their Application to Star-Branched Polymers," Macromolecules **36**, 9742–9751 (2003).
[33] Hirao, A., A. Matsuo, and T. Watanabe, "Precise Synthesis of Dendrimer-like Star-

Branched Poly (Methyl Methacrylate) S up to Seventh Generation by an Iterative Divergent Approach Involving Coupling and Transformation Reactions," Macromolecules **38**, 8701–8711 (2005).
[34] Hirao, A., K. Sugiyama, Y. Tsunoda, A. Matsuo, and T. Watanabe, "Precise Synthesis of Well-Defined Dendrimer-like Star-Branched Polymers by Iterative Methodology Based on Living Anionic Polymerization," J. Polym. Sci. Part A Polym. Chem. **44**, 6659–6687 (2006).
[35] Hirao, A., K. Sugiyama, A. Matsuo, Y. Tsunoda, and T. Watanabe, "Synthesis of Well-Defined Dendritic Hyperbranched Polymers by Iterative Methodologies Using Living/controlled Polymerizations," Polym. Int. **57**, 171–180 (2008).
[36] Hirao, A., T. Watanabe, K. Ishizu, M. Ree, S. Jin, K. S. Jin, A. Deffieux, M. Schappacher, and S. Carlotti, "Precise Synthesis and Characterization of Fourth-Generation Dendrimer-like Star-Branched Poly(methyl Methacrylate)s and Block Copolymers by Iterative Methodology Based on Living Anionic Polymerization," Macromolecules **42**, 682–693 (2009).
[37] Snijkers, F., D. Vlassopoulos, H. Lee, J. Yang, T. Chang, P. Driva, N. Hadjichristidis, and F. Snijkers, "Start-up and Relaxation of Well-Characterized Comb Polymers in Simple Shear Polymers in Simple Shear," J. Rheol. **57**, 1079–1100 (2013).
[38] Román Marín, J. M., J. K. Huusom, N. J. Alvarez, Q. Huang, H. K. Rasmussen, A. Bach, A. L. Skov, and O. Hassager, "A Control Scheme for Filament Stretching Rheometers with Application to Polymer Melts," J. Nonnewton. Fluid Mech. **194**, 14–22 (2013).
[39] Huang, Q., L. Hengeller, N. J. Alvarez, and O. Hassager, "Bridging the Gap between Polymer Melts and Solutions in Extensional Rheology," Macromolecules **48**, 4158–4163 (2015).
[40] Das, C., D. J. Read, D. Auhl, M. Kapnistos, J. den Doelder, I. Vittorias, and T. C. B. McLeish, "Numerical Prediction Of Nonlinear Rheology Of Branched Polymer Melts," J. Rheol. **58**, 737–757 (2014).
[41] Larson, R. G., "Combinatorial Rheology of Branched Polymer Melts," Macromolecules **34**, 4556–4571 (2001).
[42] Van Ruymbeke, E., C. Bailly, R. Keunings, and D. Vlassopoulos, "A General Methodology to Predict the Linear Rheology of Branched Polymers," Macromolecules **39**, 6248–6259 (2006).
[43] Milner, S. T. and T. C. B. McLeish, "Parameter-Free Theory for Stress Relaxation in Star Polymer Melts," Macromolecules **30**, 2159–2166 (1997).
[44] Blackwell, R. J., O. G. Harlen, and T. C. B. McLeish, "Theoretical Linear and Nonlinear Rheology of Symmetric Treelike Polymer Melts," Macromolecules **34**, 2579–2596 (2001).
[45] Marrucci, G., "Relaxation by Reptation and Tube Enlargement : A Model for Polydisperse Polymers," J. Polym. Sci. Polym. Phys. Ed. **23**, 159–177 (1985).
[46] Daniels, D. R., T. C. B. Mcleish, B. J. Crosby, and R. N. Young, "Molecular Rheology of Comb Polymer Melts . 1 . Linear Viscoelastic Response," Macromolecules **34**, 7025–7033 (2001).
[47] Kapnistos, M., D. Vlassopoulos, J. Roovers, and L. G. Leal, "Linear Rheology of Architecturally Complex Macromolecules : Comb Polymers with Linear Backbones," Macromolecules **38**, 7852–7862 (2005).
[48] Kirkwood, K. M., L. G. Leal, P. Driva, and N. Hadjichristidis, "Stress Relaxation of Comb Polymers with Short Branches," Macromolecules **42**, 9592–9608 (2009).
[49] Bacova, P., L. G. D. Hawke, D. J. Read, and A. J. Moreno, "Dynamics of Branched

Polymers : A Combined Study by Molecular Dynamics Simulations and Tube Theory," Macromolecules **46**, 4633–4650 (2013).
[50] Zhou, Q. and R. G. Larson, "Direct Molecular Dynamics Simulation of Branch Point Motion in Asymmetric Star Polymer Melts," Macromolecules **40**, 3443–3449 (2007).
[51] Park, S. J., P. S. Desai, X. Chen, and R. G. Larson, "Universal Relaxation Behavior of Entangled 1,4-Polybutadiene Melts in the Transition Frequency Region," Macromolecules **48**, 4122–4131 (2015).
[52] Li, S. W., H. E. Park, and J. M. Dealy, "Evaluation of Molecular Linear Viscoelastic Models for Polydisperse H Polybutadienes," J. Rheol. **55**, 1341 (2011).
[53] Bick, D. and T. McLeish, "Topological Contributions to Nonlinear Elasticity in Branched Polymers," Phys. Rev. Lett. **76**, 2587–2590 (1996).
[54] Verbeeten, W. M. H., G. W. M. Peters, and F. P. T. Baaijens, "Differential Constitutive Equations for Polymer Melts: The Extended Pom–Pom Model," J. Rheol. **45**, 823–843 (2001).
[55] Hawke, L. G. D., Q. Huang, O. Hassager, and D. J. Read, "Modifying the Pom-Pom Model for Extensional Viscosity Overshoots," J. Rheol. **59**, 995–1017 (2015).
[56] Huang, Q., S. Agostini, L. Hengeller, M. Shivokhin, N. J. Alvarez, L. R. Hutchings, and O. Hassager, "Dynamics of Star Polymers in Fast Extensional Flow and Stress Relaxation," Macromolecules **49**, 6694–6699 (2016).
[57] Snijkers, F. and D. Vlassopoulos, "Appraisal of the Cox-Merz Rule for Well-Characterized Entangled Linear and Branched Polymers," Rheol. Acta **53**, 935–946 (2014).
[58] Ianniruberto, G. and G. Marrucci, "Entangled Melts of Branched PS Behave like Linear PS in the Steady State of Fast Elongational Flows," Macromolecules **46**, 267–275 (2013).
[59] Alvarez, N. J., J. M. R. Marín, Q. Huang, M. L. Michelsen, and O. Hassager, "Creep Measurements Confirm Steady Flow after Stress Maximum in Extension of Branched Polymer Melts," Phys. Rev. Lett. **110**, 1–4 (2013).
[60] Hassager, O., K. Mortensen, A. Bach, K. Almdal, H. K. Rasmussen, and W. Pyckhout-Hintzen, "Stress and Neutron Scattering Measurements on Linear Polymer Melts Undergoing Steady Elongational Flow," Rheol. Acta **51**, 385–394 (2012).